View metadata, citation and similar papers at core.ac.uk

brought to you by CORE

provided by Loughborough University Institutional Repository

Scalable Synthesis of Multicolour Conjugated Polymer Nanoparticles via Suzuki-Miyaura Polymerisation in a Miniemulsion and Application in Bioimaging

Jonathan M. Behrendt[a, 1], Jair A. Esquivel Guzman[a], Laura Purdie[b], Helen Willcock[c, 2], John J. Morrison[a], Andrew B. Foster[a], Rachel K. O'Reilly[c], Mark C. McCairn[a], Michael L. Turner[a*]

[a] School of Chemistry, University of Manchester, Oxford Road, Manchester, M13 9PL, U.K.

[b] School of Pharmacy, University of Nottingham, University Park, Nottingham, NG7 2RD, U.K.

[c] Department of Chemistry, University of Warwick, Gibbet Hill, Coventry, CV4 7AL, U.K.

Corresponding Author

* University of Manchester. Oxford Road, Manchester M13 9PL, UK. Email: michael.turner@manchester.ac.uk Fax: +44(0)1612754273; Tel: +44(0)1612754625.

Present Addresses

[1] (J.M.B.) Cambridge Display Technology, Unit 12, Cardinal Park, Cardinal Way, Godmanchester PE29 2XG, United Kingdom.

[2] (H.W.) Department of Materials, Loughborough University, Loughborough LE11 3TU, United Kingdom.

Abstract

Suzuki cross-coupling polymerisation of aryldibromides and aryldiboronate esters in a sodium dodecyl sulfate (SDS)-stabilised miniemulsion provides a versatile and direct route to fluorescent conjugated polymer nanoparticles (CPNs). These nanoparticles have a conjugated backbone based on poly(9,9-dioctylfluorene) (PFO), however, significant structural diversity is introduced by incorporation of electron withdrawing, heterocyclic comonomers (5-50 mol. %) in order to tune the emission wavelengths from blue to far-red/near-infrared. The robust nature of the polymerisation methodology allows for rapid assessment of the relationship between polymer composition, chain morphology and optical properties of the resultant CPNs. Moreover, the CPNs (after a simple and rapid purification step) can be used directly in fluorescence-based intracellular labelling experiments (in HCT116 cells), in which they display low cytotoxicity at biologically-useful concentrations.

Keywords

conjugated polymer nanoparticles, miniemulsion, Suzuki-Miyaura polymerisation, scalable, bioimaging

1. Introduction

Conjugated polymer nanoparticles (CPNs), sometimes referred to as conjugated polymer dots, have been examined for a wide range of fluorescence-based cellular labelling and biomedical imaging applications. In vitro, CPNs display low cytotoxicity and can be internalized by cells through several active mechanisms that depend on the size and nature of the nanoparticle surface.[1-4] Recent developments include the use of CPNs for in vivo targeted bioimaging of tumours, highlighting the potential of these materials as molecular imaging probes in a clinical setting.[5-9] CPNs do not show the undesirable fluorescence

blinking behaviour and inherent toxicity associated with heavy-metal (e.g. Cd, Pb) derived quantum dots that are often used in similar applications.[10, 11] Two methods for the formation of CPNs have dominated literature reports to-date: i) nanoprecipitation, in which a dilute solution of a conjugated polymer (CP) in a water miscible, 'good solvent' (usually tetrahydrofuran) is added rapidly to a non-solvent (water),[12-14] and ii) miniemulsion, in which a solution of a CP in a non-water miscible, volatile solvent (e. g. dichloromethane) is emulsified in an aqueous solution of an appropriate surfactant, followed by solvent evaporation.[15-17] Both of these processing techniques are relatively straightforward and applicable to a range of commercially available CPs. The major limitation of these approaches is a lack of scalability: nanoprecipitation is particularly problematic in this respect in that it can only be achieved using very dilute polymer solutions and thus the resultant CPN dispersions have low solids contents (typically < 500 ppm). Miniemulsion of pre-formed CPs can be used to produce stable CPN dispersions at higher concentrations, but this approach necessitates the use of a multistep procedure in which the CP is initially prepared and isolated using conventional synthetic methods prior to subsequent dispersion in the miniemulsion.

In an effort to minimize these limitations, various research groups have developed synthetic routes to CPNs in which the polymerisation and nanoparticle formation are achieved concurrently.[7, 18-24] The various classes of light-emitting CPs from which formation of CPNs is desirable are structurally diverse and, moreover, their optical bandgap (and consequently their fluorescence emission wavelength) is directly controlled by the chemical composition of the polyaromatic backbone. Consequently, the scope of any direct synthetic route to CPNs is very much reliant on the versatility of the underlying polymerisation technique. Weder et al. pioneered this one-pot approach to CPNs, through their early report of the synthesis of hyperbranched poly(phenylene ethynylene) (PPE) nanoparticles via Sonogashira coupling of $A_2 + B_2 + A_3$ monomers (where A = bromo/iodo, B = ethynyl) in

emulsified droplets of toluene in an aqueous solution of the ionic surfactant sodium dodecylsulfate (SDS).[18] Most notably, the authors demonstrated that use of an ultrasonic bath for emulsification enabled the synthesis of fluorescent nanoparticles with average diameters ranging from 400-500 nm. The scope for heterogeneous Sonogashira polymerisation reactions to be used in the direct synthesis of PPE-based CPNs has since been considerably extended by Mecking et al.[19] Here the authors focused on A_2 + B_2 step-growth reactions, employing the same catalytic system ($Pd(PPh_3)_4$, CuI, diisopropylamine), dispersed solvent (toluene) and surfactant (SDS) as the earlier report. More rigorous sonication prior to polymerisation was found to enable the formation of smaller nanoparticles (average diameter = 60-120 nm), which were of an appropriate size for use in intracellular imaging of HeLa cells. Moreover, it was demonstrated that incorporation of varying amounts of fluorenone or pyrolopyrrole comonomers into the polymer backbone provided access to blue, green or far-red/near infrared (FR/NIR) emitting CPNs.

Suzuki coupling is widely used for the synthesis of both linear and branched CPs. Unlike Sonogashira coupling, Suzuki reactions involve aryl-aryl coupling (of aryl bromides with aryl boronic acids/boronate esters) and the resultant CPs thus have fully aromatic π-conjugated backbones. Due to the ubiquity of Suzuki coupling in CP synthesis, many appropriate, mutually-reactive A_2 and B_2 monomers (where A = bromo, B = boronic acid/boronate esters) are commercially available. There have been various attempts to develop heterogeneous Suzuki polymerisation reactions for the direct synthesis of CPNs. [21-24] Liu et al. have explored the use of a non-ionic surfactant (Tween 80) for the heterogeneous, Suzuki polymerisation reaction of either 2,7-dibromo-9,9-dioctylfluorene or 4,7-dibromo-2,1,3-benzothiadiazole with a slight excess of 9,9-dioctylfluorene-2,7-diboronic acid bis(1,3-propanediol) ester and a small amount of 1,3,5-tribromobenzene (2 mol. %).[21] These reactions provide blue or green fluorescent CPNs (average diameter = 100 – 200 nm)

comprised of CPs with a hyperbranched structure. We have recently demonstrated that when carried out at room temperature, Suzuki emulsion polymerisation reactions with Triton-X102 as surfactant produce either rod-like or spherical nanoparticles, depending on the chemical structure of the conjugated polymer.[24]

The use of ionic surfactants in heterogeneous Suzuki polymerisation has advantages for emulsion stability where higher temperatures are required and also makes surfactant removal during purification steps less challenging. Ionic surfactants typically have higher critical micelle concentrations (CMCs) and lower micellar molecular weights (MMWs) than non-ionic surfactants, rendering them readily amenable to removal by dialysis. Furthermore, ionic surfactants often have much higher cloud points than their non-ionic counterparts (usually > 100 °C). Mecking and co-workers have reported the direct synthesis of poly(9,9-dioctylfluorene) CPNs via the Suzuki polymerisation reaction of an A-B type monomer, 2-(4,4,5,5-tetramethyl-1,3,2-dioxaborolan-2-yl)-7-bromo-9,9-dioctylfluorene, in an SDS-stabilised miniemulsion using $Pd(PPh_3)_4$ as a catalyst and sodium hydroxide as base.[23]

<Scheme 1 inserted her>

Destabilisation of the miniemulsion was avoided by using the minimum amount of base (2 mol. equivalents) necessary to promote the catalytic reaction. A similar approach has since been employed for the synthesis of CPNs by reaction of 9,9-dioctylfluorene-2,7-diboronic acid bis(1,3-propane-diol) ester and 1,3,5-dibromobenzene in a miniemulsion that was stabilised by the cationic surfactant cetyl trimethylammonium bromide.[22] Both of these reports provide useful strategies for the direct synthesis of CPNs with relatively small diameters (ca. 40-150 nm), but are limited in their scope in that both reports focused on the preparation of fluorene homopolymers.

In order to demonstrate that Suzuki miniemulsion polymerisation reactions are robust, generally applicable and afford considerable structural diversity, we herein report the use of this technique for the polymerisation of a range of A_2 + B_2 type monomers. All reactions contain 50 mol. % of 2,2'-(9,9-dioctyl-9H-fluorene-2,7-diyl)bis(4,4,5,5-tetramethyl-1,3,2-dioxaborolane), **2**, as the B_2 monomer: structural variety is achieved through reaction with different A_2 comonomers to copolymers of poly(9,9-di-n-octylfluorenyl-2,7-diyl) (PFO). This approach provides access to either alternating co-polymers (with 50 mol. % of a single A_2 comonomer) or random copolymers (with varying molar ratios of two different A_2 comonomers). The latter approach gives valuable information on the optimal incorporation (mol. %) of comonomers to ensure a complete bathochromic shift in fluorescence emission in the resultant CPNs while minimising detrimental effects on quantum yield that were found to arise from increased interchain aggregation at higher levels of incorporation. The compatibility of these nanoparticles with standard cellular imaging and analysis techniques, such as microscopy and flow cytometry, has been assessed.

2. Experimental

2.1. Materials

2,7-Dibromo-9,9-dioctyl-9H-fluorene, **1**, was synthesised from 2,7-dibromofluorene (97%, Sigma Aldrich) using standard literature procedures.[25, 26] 2,2'-(9,9-Dioctyl-9H-fluorene-2,7-diyl)bis(4,4,5,5-tetramethyl-1,3,2-dioxaborolane), **2**, was prepared from **1**, again using a standard literature procedure.[27] 4,7-Dibromo-2,1,3-benzothiadiazole, **3**, was prepared in two steps from o-phenylenediamine (>99%, Sigma Aldrich) by modification of a literature method.[28] The method employed was identical save that in the first step direct extraction into dichloromethane of the intermediate, 2, 1, 3-benzothiadiazole, from acid solution was employed rather than steam distillation, and the isolated compound was then directly

brominated to give **3**. The spectroscopic data for each compound was in agreement with that reported in the literature. Amberlite XAD-2 resin, tetrakis(triphenylphosphine)palladium(0) and monomer **4** were purchased from Sigma Aldrich. All commercially sourced compounds were used as received, without further purification.

2.2. Miniemulsion Polymerisation

The following procedure for the synthesis of **NP1a** is representative of the method used to synthesise all of the CPN samples discussed. Sodium dodecyl sulfate (50.0 mg) and deionized water (20 mL) were transferred to a Schlenk tube and the resultant solution was degassed by bubbling with argon for 20 minutes. Monomers **1** (50.0 mg, 9.12 x 10^{-2} mmol) and **2** (58.6 mg, 9.12 x 10^{-2} mmol) were dissolved in toluene (1.00 mL), to which hexadecane (78 µL) was also added, and this solution was degassed for 5 minutes in the same manner. Tetrakis(triphenylphosphine)palladium(0) (2.2 mg, 1.90 x 10^{-3} mmol) was added to the monomer solution, which was then transferred to the reaction vessel. The reaction mixture was emulsified by ultrasonication (Cole Parmer 750W ultrasonicator, fitted with microtip, set to 22 % power) for 2 minutes while cooling with an ice bath. The Schlenk tube was resealed and the miniemulsion was heated to 72 °C, followed by addition of 1M aqueous sodium hydroxide solution (365 µL), and the reaction mixture was stirred for 16 hours. After cooling to room temperature, the cap of the reaction vessel was removed and the emulsion was stirred for 5 hours to remove the residual toluene. The effective conjugated polymer concentration generated in this particular miniemulsion is approx. 3500 ppm, higher than that typical achievable via nanoprecipitation.

Note: For **NP1b**, the amount of water used in the reaction was halved (10 mL) compared to the amount used for synthesis of **NP1a**. This equates to an effective conjugated polymer concentration in the resultant miniemulsion of approx. 7000 ppm. For **NP2a-c** and **NP3a-b**

the only change to the procedure described for **NP1a** is the choice of comonomers and the molar ratio of these monomers (Table 1). In each reaction, the total number of moles of the combined comonomers was 1.82×10^{-1} mmol.

2.3. Surfactant Removal

To prepare the nanoparticle dispersions for use in cellular assays, a 4 mL aliquot of the as-prepared dispersion was added to 200 mg of Amberlite XAD-2 resin (prewashed twice with deionised water) and this suspension was shaken at room temperature for one hour. The resin was removed by decantation of the aqueous nanoparticle dispersion (using a syringe with a fine needle) and a fresh batch of resin (200 mg) was subsequently added. After shaking for a further hour, the nanoparticle dispersion was similarly decanted and then filtered through glass wool to remove any residual beads of the Amberlite XAD-2.

2.4. Characterisation

2.4.1. DLS Analysis

DLS particle size analysis of the nanoparticles in water was carried out after dilution of the as-prepared aqueous nanoparticle dispersion (400 μL) with deionised water (1.6 mL) and surfactant removal (as described above, using 2 x 20 mg of Amberlite XAD-2), using a Malvern Zetasizer Nano ZS. All DLS particle size analyses were carried out at a controlled temperature of 20 °C.

2.4.2. GPC Analysis

In order to prepare THF solutions of the linear CPs that comprise **NP1a-b**, **NP2a-c** and **NP3a-b**, a 200 μL aliquot of the as-prepared nanoparticle dispersion was flocculated through addition of 1.3 mL methanol and the polymer was isolated by centrifugation (14,000 rpm, 1 minute) and decantation of the supernatant. The polymer was dried in air to remove residual

methanol before dissolving in tetrahydrofuran (1 mL) and the resultant solution was filtered through a 0.45 μm syringe filter. GPC analysis was carried out at 35 °C using a Viscotek GPCmax VE2001 solvent/sample module with 2 × PL gel 10 μm Mixed-B and PL gel 500A columns, a Viscotek VE3580 RI detector and a VE 3240 UV/VIS 50 multichannel detector. The flow rate was 1 mL/min and the system was calibrated with low polydispersity polystyrene standards in the range of 200 to 180 $\times 10^4$ g mol^{-1} from Agilent. The analysed samples contained n-dodecane as a flow marker.

2.4.3. UV/Vis and PL Analysis

For recording of absorption and emission spectra in water, the aqueous nanoparticle dispersion (as-prepared for DLS analysis, described above) was diluted with water to an optical density of between 0.5 and 1. UV-Vis absorption spectra of the nanoparticles at this concentration were recorded on a Varian Cary 55 5000UV-Vis- NIR spectrophotometer at room temperature. PL spectra were recorded on a Varian Cary Eclipse fluorimeter.

<Table 1 inserted here>

2.4.4. PLQY Analysis

All PLQY measurements were obtained using a Fluoromax-4 spectrofluorometer with integrating sphere attachment (instrument standardized with a Tungsten lamp). Nanoparticle suspensions in water were diluted to an optical density < 0.2 for measurements. Background reference measurements were obtained using water (600 μL) in 7 x 40 mm clear glass vials. Nanoparticle suspensions (600 μL) were also measured in 7 x 40 mm clear glass vials. An excitation wavelength of 390 nm was used for all samples apart from F8BT nanoparticles **NP2c**, for which the excitation wavelength was 440 nm. To calculate PLQYs, four measurements were obtained: i) background scatter (e. g. 380-400 or 430-450 nm); ii)

background fluorescence (400-760 nm); iii) sample scatter (e. g 380-400 nm or 430-450 nm); and iv) sample fluorescence (400-760 nm). Appropriate optical filters were used to avoid oversaturation of the detector during collection of scatter measurements and these filters were corrected for in the PLQY calculation. For each sample of nanoparticles, PLQY measurements were repeated in triplicate, using a fresh suspension after each set of sample scatter and sample fluorescence measurements. The reported PLQY value is therefore an average of three measurements.

2.4.5. TEM Analysis

Solutions of graphene oxide were synthesised as reported previously.[29] Aqueous solutions of graphene oxide (0.10 mg/mL) were sonicated for 30 s prior to use. Lacey carbon grids (400 Mesh, Cu) (Agar Scientific) were cleaned using air plasma from a glow-discharge system (2 min, 20 mA). The TEM grids were placed on a filter paper and one drop (≈ 0.08 mL) of the sonicated GO solution was deposited onto each grid from a height of ≈ 1 cm, allowing the filter paper to absorb the excess solution, and the grids were left to air-dry in a desiccator cabinet for ≈ 60 min. 5 μL of the nanoparticle dispersion (100 ppm) was pipetted onto a GO grid and blotted away with filter paper after 2 minutes, the grid was then left to air-dry in a desiccator cabinet for ≈ 60 min. Brightfield TEM images were captured with a transmission electron microscope (JEOL 2000FX), operating at 200 kV. Average sizes of the nanoparticles were determined from counting the sizes of 200 particles for each sample.

2.4.6. Cell Culture

HCT116, A549 and MCF-7 cells were obtained from ATCC. All cell lines were maintained in RPMI-1640 media supplemented with 10 % heat inactivated fetal calf serum and 0.2 mM L-glutamine in a humidified incubator with 5 % CO_2.

2.4.7. Viability Assay

Cells were seeded in 96 well plates at 10,000 cells per well 24 hours prior to use. Cells were incubated with particles diluted in Optimem media (Life Technologies) at the stated concentrations for 24 hours. The media was aspirated and the cells washed once in PBS. The cells were then incubated with Alamar Blue reagent (Life technologies) for 1 hour and fluorescence was measured at excitation 585 nm emission 610 nm.

2.4.8. Confocal Microscopy

HCT-116 cells were seeded on cover glass slides. After 24 hours they were incubated with particles (50 µg/ml in Optimem) for 2 hours after which time they were washed three times in cold PBS. **NP2c** samples were counterstained with CellMask™ Deep Red Plasma membrane stain (Life Technologies) and Hoechst 33342 for 5 minutes at 37 °C. Cells were fixed for 5 minutes at room temperature in 4 % paraformaldehyde-PBS prior to imaging using a LSM710 META confocal microscope (Zeiss).

2.4.9. Flow Cytometry

Cells were seeded on 6 well tissue culture plates for 24 hours. They were incubated with 50 µg/ml particles for 2 hours then washed three times in ice cold PBS. Cells were trypsinized and fixed in 4 % paraformaldehyde –PBS for 5 minutes at room temperature. Cells were resuspended in PBS and analysed by flow cytometry within 24 hours using a MoFlo XDP flow cytometer (Beckman Coulter). Flow cytometer settings were **NP1a**: 405 nm excitation, emission 417.4-482.5 nm; **NP2c**: 488 nm excitation, emission 515-543 nm; **NP3a**: 488 nm excitation, 655-685 nm emission.

<Fig. 1. inserted here>

<Fig. 2. inserted here>

3. Results and Discussion

3.1. Miniemulsion Polymerisation and Surfactant Removal

Initial efforts to develop a versatile route for the direct synthesis of CPNs by Suzuki reaction of A_2 + B_2 monomers focused on the synthesis of CPNs of PFO via copolymerisation of equimolar amounts of 2,7-dibromo-9,9-dioctyl-9H-fluorene, **1**, and 2,2'-(9,9-dioctyl-9H-fluorene-2,7-diyl)bis(4,4,5,5-tetramethyl-1,3,2- dioxaborolane), **2**. The miniemulsion reactions remain stable at dispersed/continuous phase ratios of 1:20 and 1:10. These are higher than previously reported (1:25), which has advantages in terms of potential for scale-up.[23] Previous reports showed that varying the surfactant concentration from 1 – 0.08 wt. % decreased the mean particle diameter from 85 to 39 nm.[23] In this contribution, which is primarily focused on varying the copolymer structure, a surfactant concentration close to the minimum amount necessary to provide a stable miniemulsion throughout the reaction was used, e.g. 0.25 and 0.5 wt. % for dispersed/continuous phase ratios of 1:20 and 1:10, respectively. The use of a low surfactant concentration minimised the number of purification cycles necessary for removal of free surfactant in the final dispersions. TEM analysis of **NP1a** and **NP1b** (produced with dispersed/continuous phase ratios of 1:20 and 1:10 respectively), showed that nanoparticles obtained by this method generally have a spherical morphology (see Figure 1). There is some disparity in size between the distributions obtained via DLS and TEM for all samples (see Table 1), due to the relatively polydisperse nature of the samples. However, both methods are in agreement that the majority of particles present in all samples are below 100 nm in diameter and thus readily amendable to entry into cells by active mechanisms, e.g. endocytosis.[30] Moreover, CPNs prepared by precipitation with a similar level of polydispersity within this size regimen have been successfully employed in real-time sentinel lymph node mapping in vivo.[7]

Purification of the CPNs for application in cellular imaging requires removal of the organic solvent (toluene) and free surfactant. Removing the lid of the reaction vessel and stirring at room temperature for 5 hours achieved the former, while the latter can be achieved by an exhaustive dialysis of the dispersion (7 days, changing the water twice daily). However, dialysis is both time-consuming, causing a considerable bottleneck in CPN production, and expensive, hence an alternative strategy was investigated. In protein purification detergent removal (ionic and non-ionic surfactants) can be achieved by the use of a porous, hydrophobic polystyrene resin, Amberlite XAD-2.[31, 32] It was found that for the CPNs prepared in this work it was possible to remove both the residual toluene and the SDS to a final level that is below the surfactant CMC by simply shaking the crude nanoparticle suspension (as a 5-fold dilution) with 1 wt. % of Amberlite XAD-2 for 15 minutes and then repeating this process with a fresh batch of resin. Analysis of the samples purified by this method by DLS shows no detrimental effects on the CPN size or polydispersity (Table 1). Unlike dialysis, purification using the resin does not remove the aqueous base (sodium hydroxide) employed in the polymerisation, however it was at a sufficiently low level that the as-purified CPN suspension could be added directly to biological buffer solutions without the need for further purification. Using this approach it is possible to produce sub-100 nm PFO nanoparticles at high concentrations (**NP1b**, Table 1), however these more concentrated samples (1:10, dispersed/continuous) tended to flocculate after surfactant removal by treatment with Amberlite XAD-2 resin upon standing for several hours. Hence in all subsequent copolymerisation reactions a dispersed/continuous phase ratio of 1:20 was employed as these dispersions can be stored for several months following surfactant removal, without dilution.

Measurement of UV/vis and PL spectra of **NP1a** in dilute aqueous suspension, indicated that the PFO adopts a mixture of glassy phase (disordered) and β-phase (ordered) chain

morphologies within the nanoparticles (Figure 2). The β-phase is an ordered form of PFO in which the backbones of neighbouring polymer chains are planarized with respect to each other.[33] This is consistent with the findings of a number of previous reports in which aqueous dispersions of PFO nanoparticles have been processed from (or annealed with) a "good" solvent.[34, 35] The photoluminescence quantum yield (PLQY) of **NP1a** in water (38 %) is similar to values reported for PFO NPs prepared by other methods.[23, 34] In order to assess the degree of polymerisation obtained by Suzuki polymerisation in a miniemulsion, small aliquots of the as-made CPN suspensions were flocculated through addition of methanol and the molecular weight of the isolated polymers (in THF) was determined by gel permeation chromatography (Table 1). The molecular weights of PFO recovered from **NP1a** and **NP1b** emulsions (M_n = 1.4 – 1.5 x 10^4 g mol^{-1}) compared favourably with those produced by reaction of an A-B monomer in the earlier report (9.0 x 10^3 – 2.3 x 10^4 g mol^{-1}),[23] indicating that A_2 + B_2 reactions can provide an acceptably high degree of polymerisation while providing the possibility of vastly expanding the structural diversity.

3.2. Green-Emitting CPNs

The emission wavelength of fluorene polymers can be tuned through copolymerisation of fluorene with various electron withdrawing co-monomers.[36, 37] Miniemulsion co-polymerisation of dioctyl fluorene monomers **1** and **2** with benzothiadiazole monomer **3** gave CPN dispersions, **NP2a-c**, that luminesce primarily in the green (Table 2). **NP2a** and **NP2b** are comprised of random copolymers, synthesised by reaction of **1** and **2** with 5 and 10 mol. % of **3**, respectively. The UV/vis absorption spectra of **NP2** are similar to those of **NP1** (Figure 3) due to the relative abundance of fluorene-fluorene segments in these materials. The secondary absorption peak observed at 437 nm for **NP2** shows that the polymers in these nanoparticles retain the ability to form the more ordered β-phase conformation, despite the

incorporation of small amounts of the benzothiadiazole units.[38] The absorbance of the fluorene-benzothiadiazole segments in **NP2** is observed as a broad shoulder that partially overlaps with the β-phase absorption and that extends to around 500 nm (Figure 3a). The PL emission of these copolymers (exciting at 390 nm) is almost exclusively derived from the relatively few fluorene-benzothiadiazole chain segments, as a result of efficient Förster Resonance Energy Transfer (FRET) between these and the fluorene-fluorene segments (Figure 3b). As a result, the effective Stokes shift for both samples is large (154 nm). Increasing the amount of benzothiadiazole monomer 3 from 5 to 10 mol. % resulted in a significant increase in the PLQY (Table 2) of the resultant nanoparticles, **NP2a** and **NP2b**, with the value for the latter (56 %) being much higher than those typically reported for green emitting CPNs.

<Fig. 3. inserted here>

<Fig. 4. inserted here>

This is analogous to the recent findings of McNeill et al., who report that CPNs comprised of blends of PFBT and MEH-PPV have a higher PLQY than CPNs comprised of PFBT alone.[39] Considering the relative complexity of the three monomer reaction, the observed polymer molecular weights (1.3-1.4 x 10^4 g mol^{-1}, Table 1) are encouraging, highlighting the robustness and efficiency of the miniemulsion polymerisation reactions. Polymerisation of a 1:1 molar ratio of **2** and **3** gave CPN dispersion **NP2c**, consisting of the well-studied alternating co-polymer F8BT.[36] The broad and featureless UV/vis and PL spectra (Figure 4) and moderate quantum efficiency (12 %) for **NP2c** are consistent with previous examples of F8BT CPNs that have been prepared by nanoprecipitation.[14] Incorporation of relatively small amounts (5-10 %) of benzothiadiazole into a random co-polymer based on PFO gives

green-emitting CPNs with significantly higher quantum efficiencies than CPNs of the exactly alternating co-polymer (F8BT).

<Table 2 inserted here>

<Fig. 5. Inserted here>

3.3. FR-NIR Emitting CPNs

In order to facilitate their use for in vivo imaging applications, there is currently considerable focus on the development of CPNs that emit in the FR/NIR region.[5-9] However, this remains a considerable challenge due to the limited solubility of low bandgap conjugated polymers and their tendency to aggregate in the solid state. The former characteristic renders these polymers less suitable for post-polymerisation fabrication into CPNs via nanoprecipitation and the latter significantly impacts upon the PLQY of the resultant nanomaterials.[9] Incorporation of the thiophene-benzothiadiazole-thiophene monomer 4 (1 – 35 mol. %) into PFO-based random copolymers in a conventional solution-based Suzuki coupling polymerisation has been shown to produce materials that display FR/NIR solid state emission when deposited as thin films.[37] Suzuki miniemulsion polymerisation reactions were carried out using **1** and **2** as comonomers, with 5 and 10 mol. % of **4** to give nanoparticle dispersions **NP3a** and **NP3b**, respectively. It was not possible to incorporate higher loadings of **4** into these dispersions due to the limited solubility of **4** in toluene at room temperature (the temperature at which the emulsification step is performed). In the case of **NP3b**, it was observed that a small amount of monomer **4** had precipitated during emulsification, and hence the maximum possible mol. % for incorporation of this comonomer into CPNs by this method lies between 5 and 10 mol. %. The precipitation of monomer **4** resulted in a reduction in the molecular weight of the polymer (5.7×10^3 g mol^{-1}) contained within these nanoparticles, when compared with those produced in the other miniemulsion

reactions (see Table 1). GPC analysis of the polymer from **NP3a** indicated a number average molecular weight of 1.2 x 10^4 g mol^{-1}, corresponding to a degree of polymerisation of around 30 and therefore an average of 3 segments derived from monomer 4 per chain. UV/vis absorption spectra of **NP3a** and **NP3b** indicated that the more abundant fluorene-fluorene segments of the polymer chains can adopt glassy phase and β-phase conformations (Figure 5a). The β-phase absorption is significantly lower for composition **NP3b** than **NP3a**. The absorption spectra also have a broad absorption peak with a maximum at 529 nm, associated with the less abundant, lower bandgap segments derived from monomer **4**. The emission spectra of **NP3a** and **NP3b** exhibited primarily red fluorescence (λ_{em} = 630 nm, exciting at 390 nm), with a significant amount of this fluorescence encompassing the FR/NIR region (Figure 5b). Unlike the green-emitting CPNs discussed above, in which complete energy transfer from the blue to green segments is observed in all cases, **NP3a** and **NP3b** both exhibit a small amount of fluorescence in the blue region, corresponding to emission from segments of β-phase PFO. Previous attempts to form efficient FR/NIR CPNs have focused on the nanoprecipitation of poly[(9,9-dihexylfluorenyl-co-2,1,3-benzothiadiazole)-co-4,7-di(thiophen-2-yl)-2,1,3-benzothiadiazole (PFBTDBT), in which the lower energy fluorene-benzothiadiazole (green-emitting) segments have a better overlap with the higher energy, red-segments than the fluorene-fluorene segments (blue-emitting) segments found in **NP3**.[5] Despite evidence of some blue emission, **NP3a** has a high PLQY (34 %) by comparison with alternative FR/NIR nanoparticles and are thus promising candidates for in vivo bioimaging applications. **NP3b**, with 10 mol. % of monomer **4**, has a slightly lower PLQY (19 %). Factors that may contribute to the lower efficiency of **NP3b** when compared to **NP3a** are the lower molecular weight of the CP chains in **NP3b** and the increased interchain aggregation caused by the higher mol. % of red-emitting segments. This is evidenced by the reduced amount of PFO β-phase observed in the UV/vis spectrum of **NP3b** (Figure 5b).

<Fig. 6. inserted here>

<Fig. 7. inserted here>

<Fig. 8. inserted here>

3.4. Cellular Imaging and Cytotoxicity Assays

The suitability of nanoparticle dipersions **NP1a**, **NP2c** and **NP3a** (blue, green and red emitting, respectively) for bioimaging was tested in 2D cell cultures. Each type of nanoparticle was shown to be detectable by flow cytometry at 50 µg/mL after a 2 hour incubation, demonstrating the potential to utilize these materials for FACS analysis experiments (Figure 6). Confocal microscopy revealed rapid internalisation of the CPNs into HCT116 cells in all cases, with a largely perinuclear localisation (Figure 7). However **NP3a** showed significant bleed though into blue, green and red channels making them impractical for multiplexing with many standard imaging reagents such as Hoechst 33342 and DAPI. In contrast, **NP2c** was compatible with reagents including Hoechst 33342, DAPI, CellMask™ Deep Red Plasma membrane (Figure 7) and red fluorescent protein (RFP) (data not shown) demonstrating that it is a good candidate for use in microscopy studies. The cytotoxicity of nanoparticles **NP1a**, **NP2c** and **NP3a** was tested using the Alamar Blue assay. After incubation for 24 hours the particles reduced viability by a maximum of 25 % of untreated controls (Table 3). At higher concentrations the viability dropped further (Figure 8) however such high concentrations were well beyond those necessary for bioimaging purposes.

<Table 3. inserted here>

4. Conclusions

We have demonstrated the wider utility of Suzuki emulsion polymerisation for the direct synthesis of CPNs with tunable fluorescence emission. Their useful optical properties, such

as high PLQYs, and small size (< 100 nm) render these nanoparticles suitable for use in biological applications, such as cellular imaging and sorting via fluorescence microscopy and flow cytometry. The methodology developed is straightforward in terms of both synthesis and purification and more readily scalable than many previously reported methods for producing CPNs. Through developing a deeper understanding of the mechanism of Suzuki emulsion polymerisation reactions and, in particular, the factors that control particle size, and use of biocompatible surfactants, one pot synthesis of CPNs has the potential to supersede current indirect methodologies (e. g. nanoprecipitation) and to support the wider use of these materials in biomedical imaging.

References

[1] L.P. Fernando, P.K. Kandel, J. Yu, J. McNeill, P.C. Ackroyd, K.A. Christensen, Biomacromolecules, 11 (2010) 2675-2682.

[2] J. Lee, M. Twomey, C. Machado, G. Gomez, M. Doshi, A.J. Gesquiere, J.H. Moon, Macromolecular Bioscience, 13 (2013) 913-920.

[3] M. Green, P. Howes, C. Berry, O. Argyros, M. Thanou, Proceedings of the Royal Society A: Mathematical, Physical and Engineering Sciences, 465 (2009) 2751-2759.

[4] R. Ahmad Khanbeigi, T.F. Abelha, A. Woods, O. Rastoin, R.D. Harvey, M.-C. Jones, B. Forbes, M.A. Green, H. Collins, L.A. Dailey, Biomacromolecules, 16 (2015) 733-742.

[5] D. Ding, J. Liu, G. Feng, K. Li, Y. Hu, B. Liu, Small, 9 (2013) 3093-3102.

[6] K. Li, D. Ding, D. Huo, K.-Y. Pu, N.N.P. Thao, Y. Hu, Z. Li, B. Liu, Advanced Functional Materials, 22 (2012) 3107-3115, S3107/3101-S3107/3107.

[7] S. Kim, C.-K. Lim, J. Na, Y.-D. Lee, K. Kim, K. Choi, J.F. Leary, I.C. Kwon, Chemical Communications (Cambridge, United Kingdom), 46 (2010) 1617-1619.

[8] C. Wu, S.J. Hansen, Q. Hou, J. Yu, M. Zeigler, Y. Jin, D.R. Burnham, J.D. McNeill, J.M. Olson, D.T. Chiu, Angewandte Chemie, International Edition, 50 (2011) 3430-3434, S3430/3431-S3430/3414.

[9] J. Liu, G. Feng, D. Ding, B. Liu, Polymer Chemistry, 4 (2013) 4326-4334.

[10] A.L. Koner, D. Krndija, Q. Hou, D.J. Sherratt, M. Howarth, ACS Nano, 7 (2013) 1137-1144.

[11] M.C. Mancini, B.A. Kairdolf, A.M. Smith, S. Nie, Journal of the American Chemical Society, 130 (2008) 10836-10837.

[12] C. Szymanski, C. Wu, J. Hooper, M.A. Salazar, A. Perdomo, A. Dukes, J. McNeill, Journal of Physical Chemistry B, 109 (2005) 8543-8546.

[13] C. Wu, C. Szymanski, J. McNeill, Langmuir, 22 (2006) 2956-2960.

[14] C. Wu, B. Bull, C. Szymanski, K. Christensen, J. McNeill, ACS Nano, 2 (2008) 2415-2423.

[15] K. Landfester, R. Montenegro, U. Scherf, R. Guntner, U. Asawapirom, S. Patil, D. Neher, T. Kietzke, Advanced Materials (Weinheim, Germany), 14 (2002) 651-655.

[16] K. Li, R. Zhan, S.-S. Feng, B. Liu, Analytical Chemistry (Washington, DC, United States), 83 (2011) 2125-2132.

[17] T. Kietzke, D. Neher, K. Landfester, R. Montenegro, R. Guentner, U. Scherf, Nature Materials, 2 (2003) 408-412.

[18] E. Hittinger, A. Kokil, C. Weder, Angewandte Chemie, International Edition, 43 (2004) 1808-1811.

[19] J. Pecher, J. Huber, M. Winterhalder, A. Zumbusch, S. Mecking, Biomacromolecules, 11 (2010) 2776-2780.

[20] M.C. Baier, J. Huber, S. Mecking, Journal of the American Chemical Society, 131 (2009) 14267-14273.

[21] R. Wang, C. Zhang, W. Wang, T. Liu, Journal of Polymer Science, Part A: Polymer Chemistry, 48 (2010) 4867-4874.

[22] H. Li, X. Wu, B. Xu, H. Tong, L. Wang, RSC Advances, 3 (2013) 8645-8648.

[23] C. Negele, J. Haase, A. Leitenstorfer, S. Mecking, ACS Macro Letters, 1 (2012) 1343-1346.

[24] D. Muenmart, A.B. Foster, A. Harvey, M.-T. Chen, O. Navarro, V. Promarak, M.C. McCairn, J.M. Behrendt, M.L. Turner, Macromolecules (Washington, DC, United States), 47 (2014) 6531-6539.

[25] R. Grisorio, P. Mastrorilli, C.F. Nobile, G. Romanazzi, G.P. Suranna, D. Acierno, E. Amendola, Macromolecular Chemistry and Physics, 206 (2005) 448-455.

[26] M.R. Craig, M.M. de Kok, J.W. Hofstraat, A.P.H.J. Schenning, E.W. Meijer, Journal of Materials Chemistry, 13 (2003) 2861-2862.

[27] S.Y. Cho, A.C. Grimsdale, D.J. Jones, S.E. Watkins, A.B. Holmes, Journal of the American Chemical Society, 129 (2007) 11910-11911.

[28] Y. Jin, Y. Kim, S.H. Kim, S. Song, H.Y. Woo, K. Lee, H. Suh, Macromolecules (Washington, DC, United States), 41 (2008) 5548-5554.

[29] N.R. Wilson, P.A. Pandey, R. Beanland, R.J. Young, I.A. Kinloch, L. Gong, Z. Liu, K. Suenaga, J.P. Rourke, S.J. York, J. Sloan, ACS Nano, 3 (2009) 2547-2556.

[30] J. Rejman, V. Oberle, I.S. Zuhorn, D. Hoekstra, Biochemical Journal, 377 (2004) 159-169.

[31] P.S.J. Cheetham, Analytical Biochemistry, 92 (1979) 447-452.

[32] M. Hiraide, T. Shima, H. Kawaguchi, Analytical Sciences, 10 (1994) 505-507.

[33] A. Monkman, C. Rothe, S. King, F. Dias, Advances in Polymer Science, 212 (2008) 187-225.

[34] C. Wu, J. McNeill, Langmuir, 24 (2008) 5855-5861.

[35] J.M. Behrendt, A.B. Foster, M.C. McCairn, H. Willcock, R.K. O'Reilly, M.L. Turner, Journal of Materials Chemistry C: Materials for Optical and Electronic Devices, 1 (2013) 3297-3304.

[36] Y. He, S. Gong, R. Hattori, J. Kanicki, Applied Physics Letters, 74 (1999) 2265-2267.

[37] Q. Hou, Y. Xu, W. Yang, M. Yuan, J. Peng, Y. Cao, Journal of Materials Chemistry, 12 (2002) 2887-2892.

[38] D.W. Bright, F.B. Dias, F. Galbrecht, U. Scherf, A.P. Monkman, Advanced Functional Materials, 19 (2009) 67-73.

[39] X. Wang, L.C. Groff, J.D. McNeill, Journal of Physical Chemistry C, 118 (2014) 25731-25739.

Figure Captions

Scheme 1. Selection of monomers employed in miniemulsion polymerisation reactions and resultant copolymers from which CPNs are comprised.

Table 1. Composition, particle size and copolymer molecular weight of CPNs synthesized via Suzuki polymerisation in a miniemulsion.

Fig. 1. TEM of PFO nanoparticles prepared with dispersed/continuous phase ratios of 1:20, **NP1a**, and 1:10, **NP1b** (scale bar = 100 nm).

Fig. 2. UV/vis and PL spectra (λ_{ex} = 390 nm) of **NP1a** in water.

Fig. 3. a) UV/vis and b) PL emission spectra (λ_{ex} = 390 nm) of **NP2a** and **NP2b** in water.

Fig. 4. UV/vis and PL emission spectra (λ_{ex} = 465 nm) of **NP2c** in water.

Table 2. Optical properties of CPNs in water.

Fig. 5. a) UV/vis and b) PL emission spectra (λ_{ex} = 390 nm) of **NP3a** and **NP3b** in water.

Fig. 6. Flow cytometric analysis: HCT116 cells incubated with 50 ug/ml of nanoparticles **NP1a**, **NP2c** or **NP3a** for 2 hours. Cell only: filled histogram; nanoparticle incubated cells: unfilled histogram. Calculated % of nanoparticle-labelled cells shown in each case.

Fig. 7. Confocal microscopy of particles in HCT116 cells. After a 2 hour incubation cells were either fixed (**NP1a**, **NP3a**) or stained with Hoechst 33342 and CellMask™ Deep Red Plasma membrane prior to fixing (**NP2c**) and visualisation by confocal microscopy (Scale bar = 10 μm). **NP1a**: particles-blue; **NP2c**: nucleus-blue, particles-green, plasma membrane-red; **NP3a**: particles-red.

Fig. 8. Cytotoxicity of particles in three cell lines. Cells HCT116, MCF7, A549 were incubated with particles at the stated concentrations for 24 hours after which time the cell viability was measured using Alamar blue assay. N=4, error bar SD.

Table 3. Mean cell viability after 24 hour incubation with 50 µg/ml of particles.

Schemes and Figures

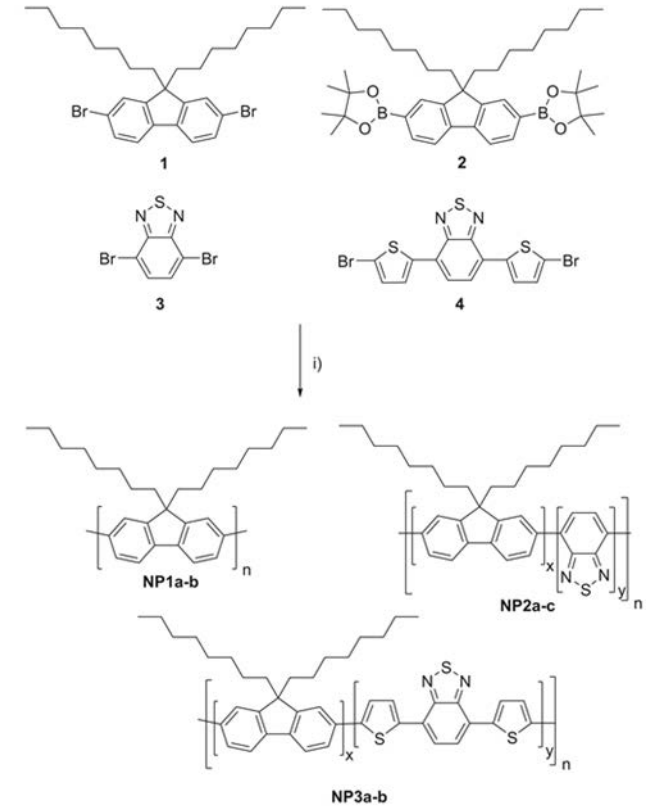

i) toluene, n-hexadecane, NaOH, $Pd(PPh_3)_4$, sodium dodecylsulfate, water, 72 °C, 16 hr

Scheme 1

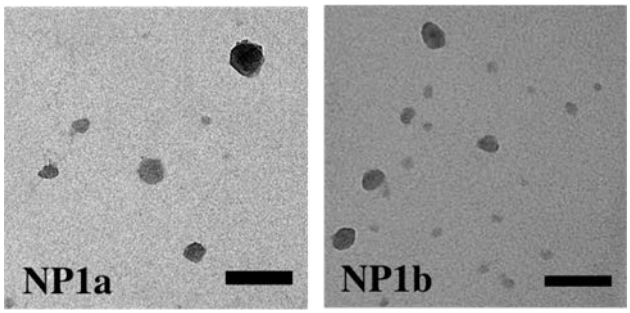

Fig. 1.

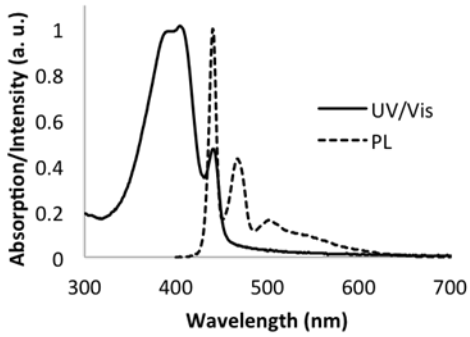

Fig. 2.

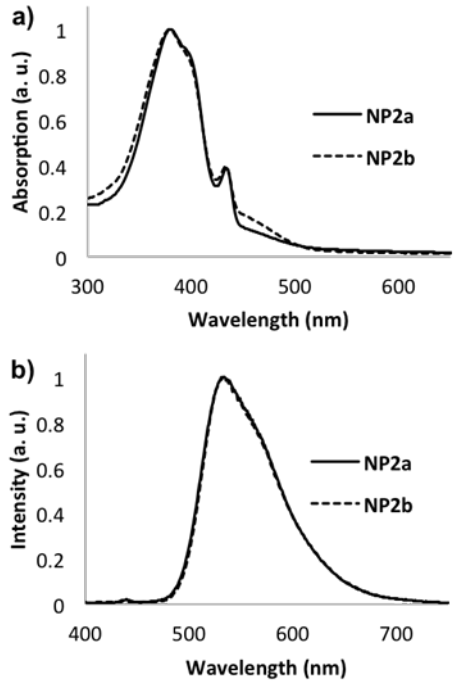

Fig. 3.

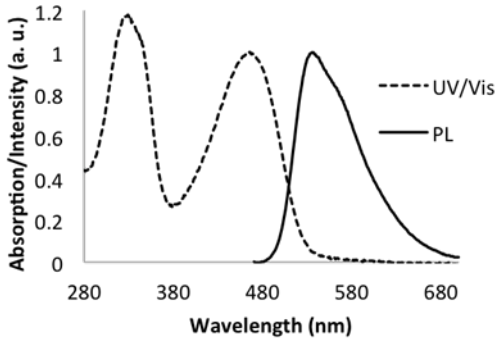

Fig. 4.

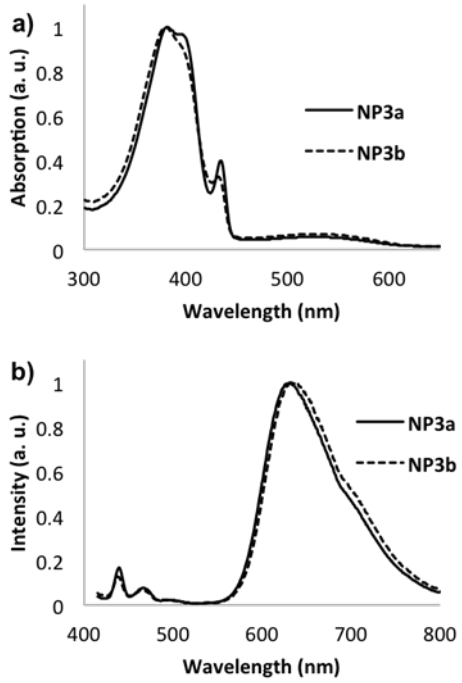
a)
Absorption (a. u.)
1
0.8
0.6
0.4
0.2
0
300
400
500
600
Wavelength (nm)
NP3a
NP3b
b)
Intensity (a. u.)
1
0.8
0.6
0.4
0.2
0
400
500
600
700
800
Wavelength (nm)
NP3a
NP3b

Fig. 5.

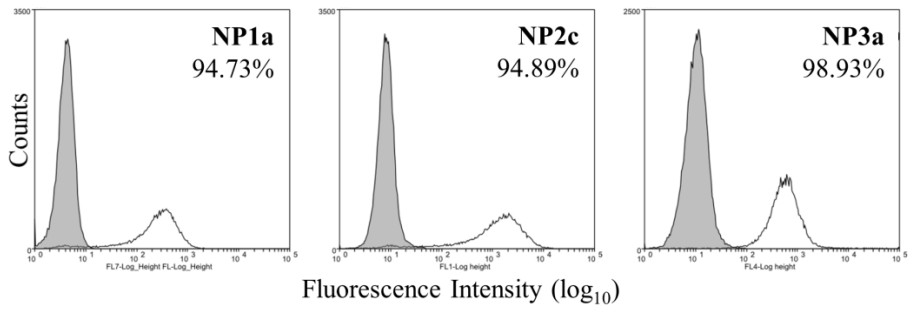
NP1a
94.73%
NP2c
94.89%
NP3a
98.93%
Counts
Fluorescence Intensity (log10)

Fig. 6.

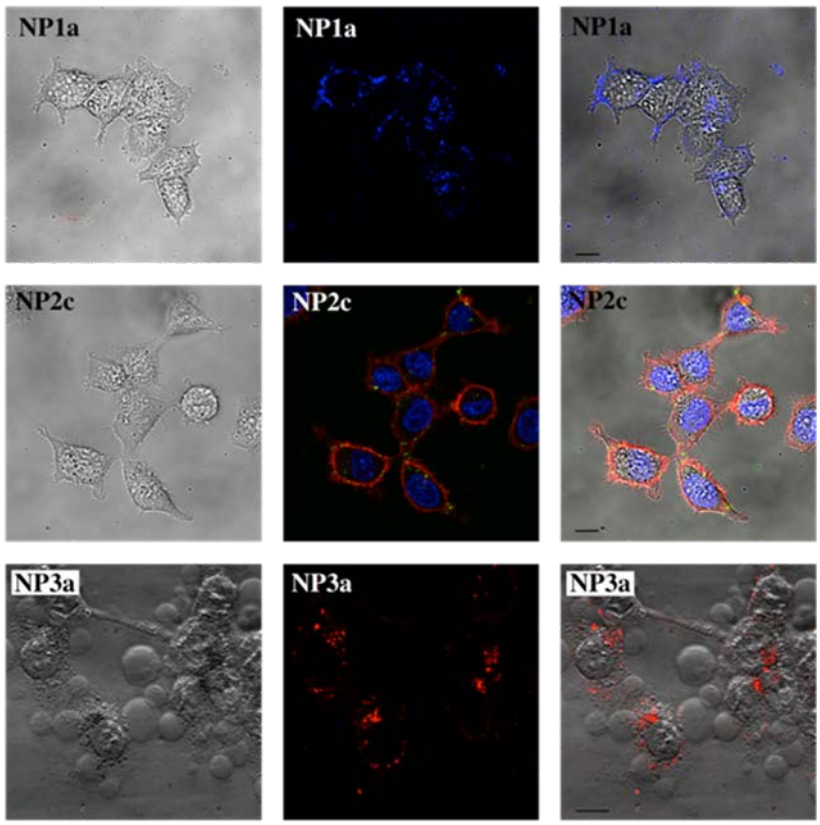
NP1a
NP1a
NP1a
NP2c
NP2c
NP2c
NP3a
NP3a
NP3a

Fig. 7.

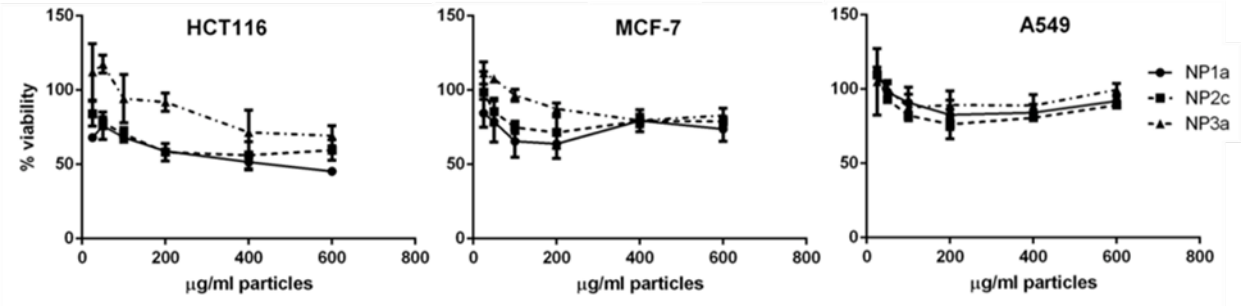
HCT116
MCF-7
A549
% viability
µg/ml particles
µg/ml particles
µg/ml particles
NP1a
NP2c
NP3a
0
50
100
150
0
200
400
600
800

Fig. 8.

Tables

Table 1

Sample code	Co-monomers	Co-monomer ratio (mol. %)	D_{DLS}[a] (nm)	PdI[b]	D_{TEM}[c] (nm)	M_n[d] (g mol^{-1})	M_w/M_n[d]
NP1a	1 + 2	50 : 50	71	0.16	23 ± 12	1.4×10^4	2.4
NP1b[e]	1 + 2	50 : 50	43 (35%), 13 (65%)[f]	0.20	19 ± 9	1.5×10^4	2.4
NP2a	1 + 2 + 3	45 : 50 : 5	45	0.17	24 ± 15	1.3×10^4	2.9
NP2b	1 + 2 + 3	40 : 50 : 10	28	0.16	21 ± 8	1.4×10^4	2.8
NP2c	2 + 3	50 : 50	73	0.16	23 ± 15	9.4×10^3	2.3
NP3a	1 + 2 + 4	45 : 50 : 5	55	0.19	25 ± 11	1.2×10^4	1.9
NP3b	1 + 2 + 4	40 : 50 : 10	59 (75%), 25 (25%)[f]	0.17	21 ± 11	5.7×10^3	3.4

a Mean diameter by number; b polydispersity index for the Gaussian size distribution measured *via* DLS; c mean diameter determined measuring 200 particles from TEM images; d molecular weight of polymer chains that comprise the nanoparticles following flocculation, centrifugation and dissolution in THF; e this sample was prepared with a dispersed/continuous phase ratio of 1:10, while this ratio was 1:20 for all other samples; f biomodal size distribution indicated for this sample.

Table 2

Sample code	λ_{max} (nm)	λ_{em} (nm)	ϕ (%)
NP1a	405	440	38 ± 2
NP1b	405	440	23 ± 2
NP2a	380	534	41 ± 3
NP2b	379	534	56 ± 1
NP2c	334, 466	537	12 ± 1
NP3a	382	631	34 ± 3
NP3b	380	633	19 ± 1

Table 3

Cells	NP1a	NP2c	NP3a
A549	98 %	93 %	100 %
HCT116	76 %	78 %	117 %
MCF7	79 %	86 %	108 %